Supplementary Information (SI) for Materials Horizons.
This journal is © The Royal Society of Chemistry 2026

Supplementary Information

Tellurium-Free GeSbSe Thin Film for Reliable Selector-Only Memory Operation

Inchan Oh[a,1], Won Hee Jeong[a,1], Jaeho Jung[b], Min Kyu Yang[c,*], and Gun Hwan Kim[a,b,*]

[a] Department of System Semiconductor Engineering, Yonsei University, Seoul 03722, Republic of Korea

[b] Department of Materials Science and Engineering, Yonsei University, Seoul 03722, Republic of Korea

[c] Department of Artificial Intelligence Semiconductor Engineering, Sahmyook University, Seoul 01795, Republic of Korea

[*] Corresponding authors.

[1]These authors contributed equally to this work

E-mail addresses: dbrophd@syu.ac.kr (M. K. Yang) and kgh@yonsei.ac.kr (G.H. Kim)

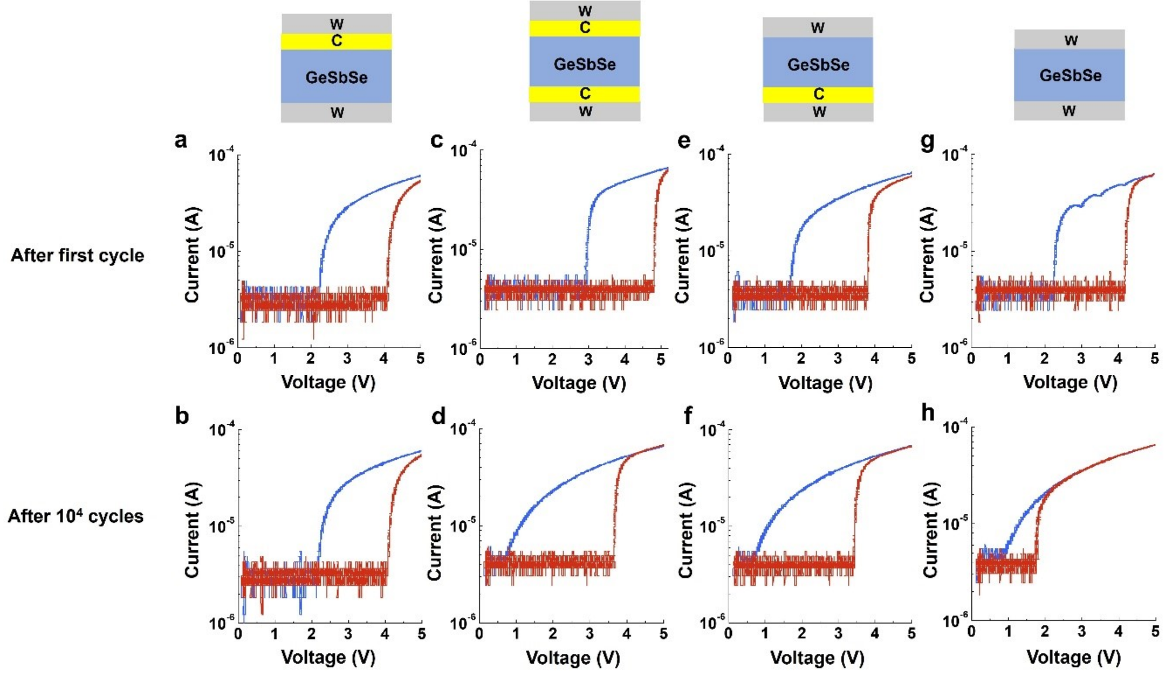

Fig. S1 PIV measurement is operated for 4 GSS SOM devices with different carbon layer positions. 1 cycle represents the alternating positive and negative write pulses. Each PIV results show before and after 10^4 write pulses cycles of the device deposited C layers (a-b) only between TE and active layer, (c-d) both TE and BE sides, (e-f) only between BE and active layer, and (g-h) no C layers.

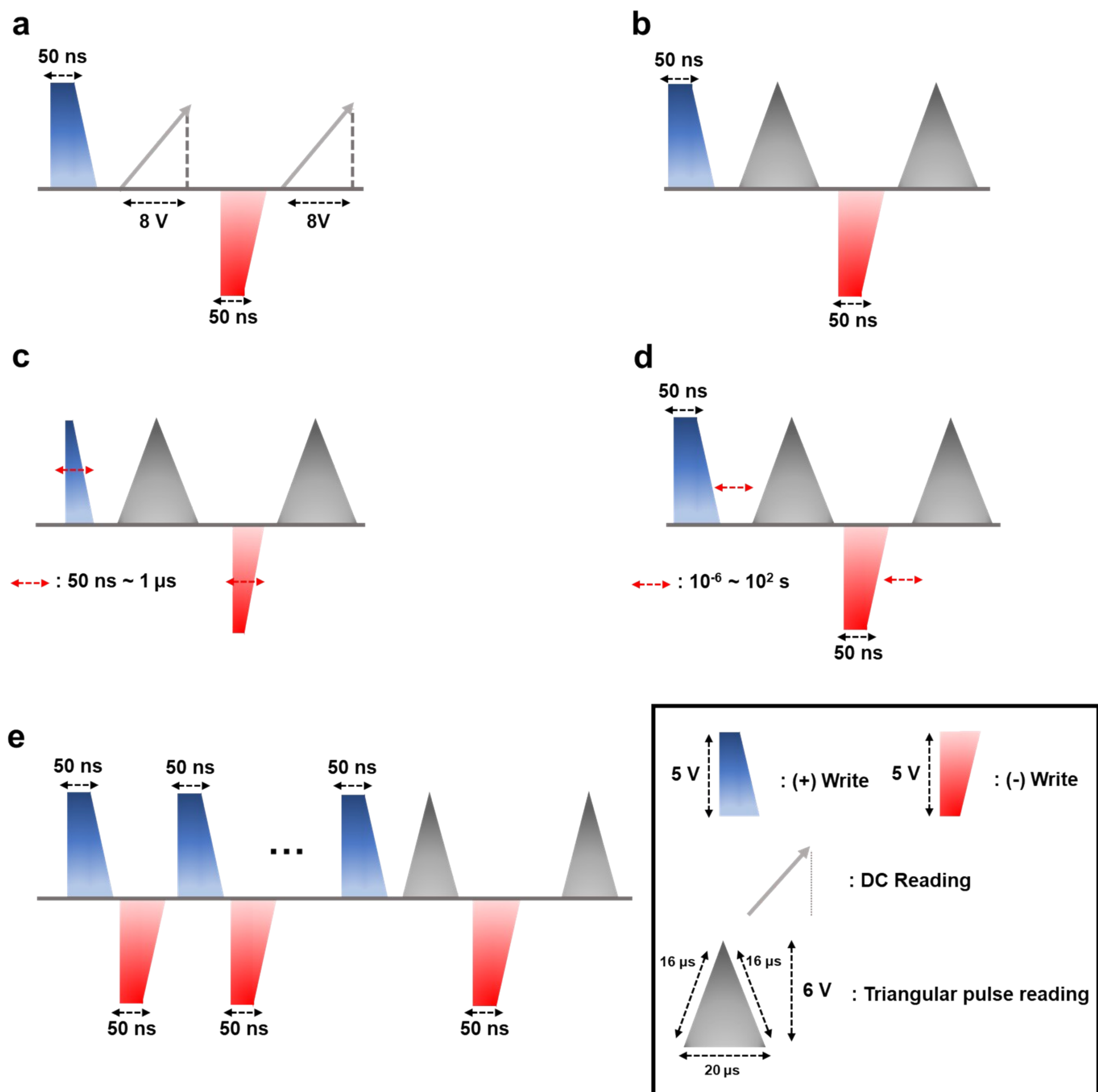

Fig. S2 (a) Applied voltage scheme for SOM *I-V* measurements. For each V_{th} state, writing was programmed by pulses, while verification was operated using DC *I-V* measurements. (b) Schematic of PIV measurement with triangular pulse reading process. (c) PIV measurement expression for speed measurement, varying the write pulse width from 50 ns to 1 μs. (d) PIV schematic for V_{th} drift measurement, ranging the delay time from 10^{-6} to 10^{2} s. Schematics for (e) endurance test, which several positive and negative write pulse cycles were applied.

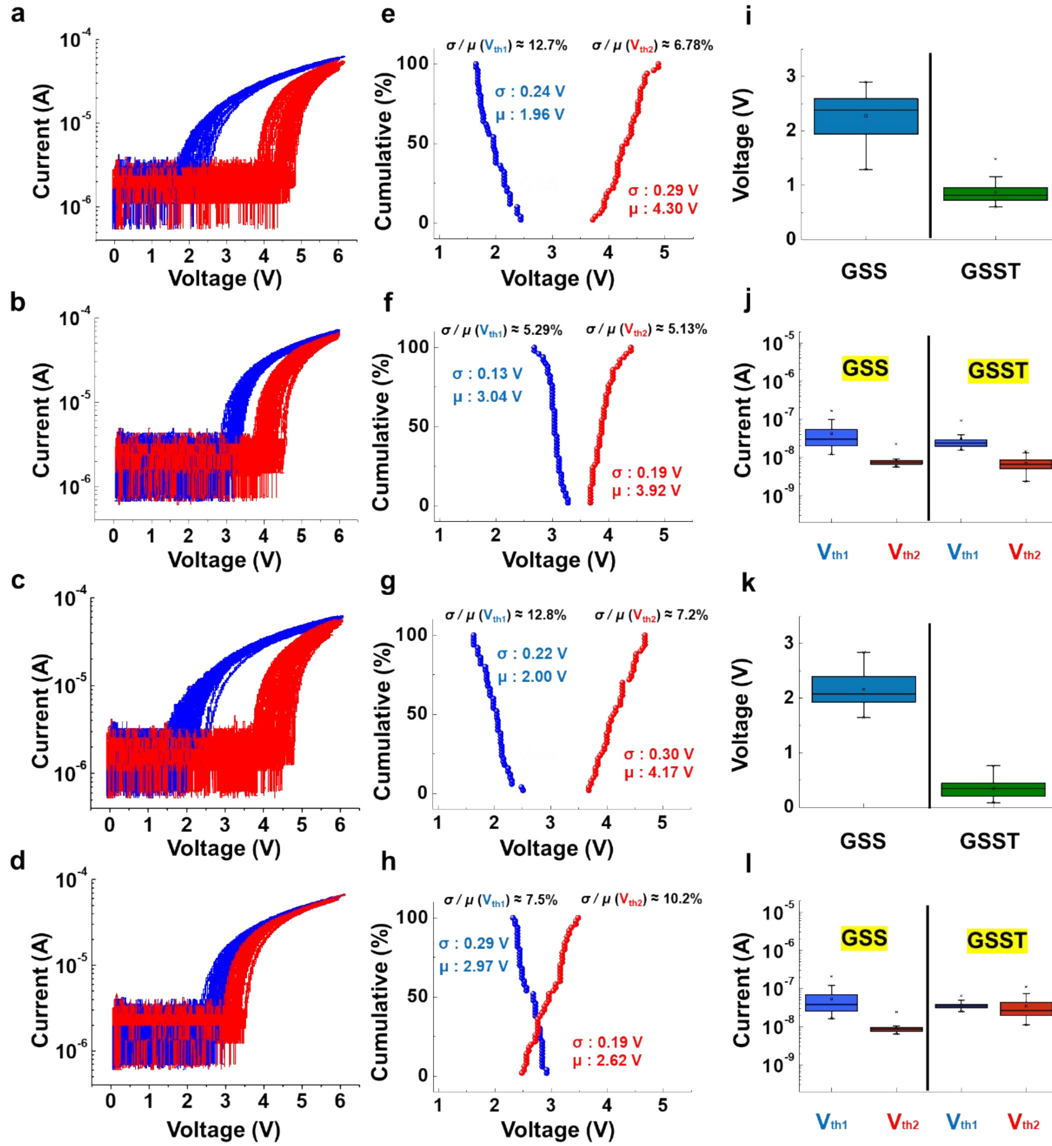

Fig. S3 Statistical evaluation of GSS and GSST SOM devices based on 50-cycle PIV measurements. (a–d) Overlaid PIV curves from 50 cycles (5 cycles × 10 cells) for (a) fresh GSS, (b) fresh GSST, (c) GSS after 10^5 write pulse cycles, and (d) GSST after 10^5 write pulse cycles. (e–h) Coefficient of variation (CV = σ/μ, σ = Standard deviation, μ = Mean value) of V_{th1} and V_{th2} for (e) fresh GSS, (f) fresh GSST, (g) cycled GSS, and (h) cycled GSST. Box plots of the read window margin (RWM) for (i) fresh and (k) cycled devices, respectively. Box plots of the off-leakage current for (j) fresh and (l) cycled devices, respectively.

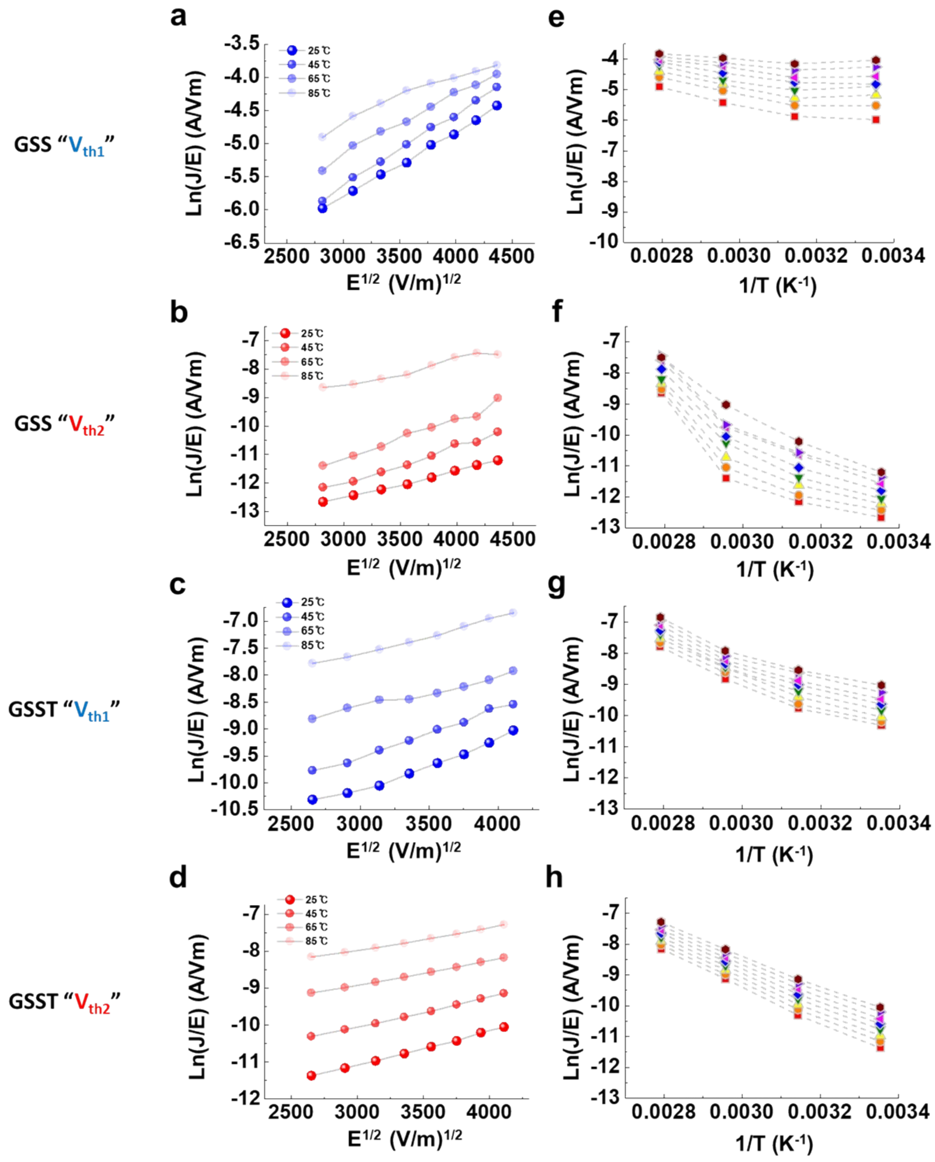

Fig. S4 (a-d) Plots representing the relationship between ln(J/E) and $E^{1/2}$ and (e-h) plots representing the relationship between ln(J/E) and $1/T$ extracted from the 0.5-1.2 V of DC I-V curves for each V_{th1} and V_{th2} states of GSS and GSST SOM devices.

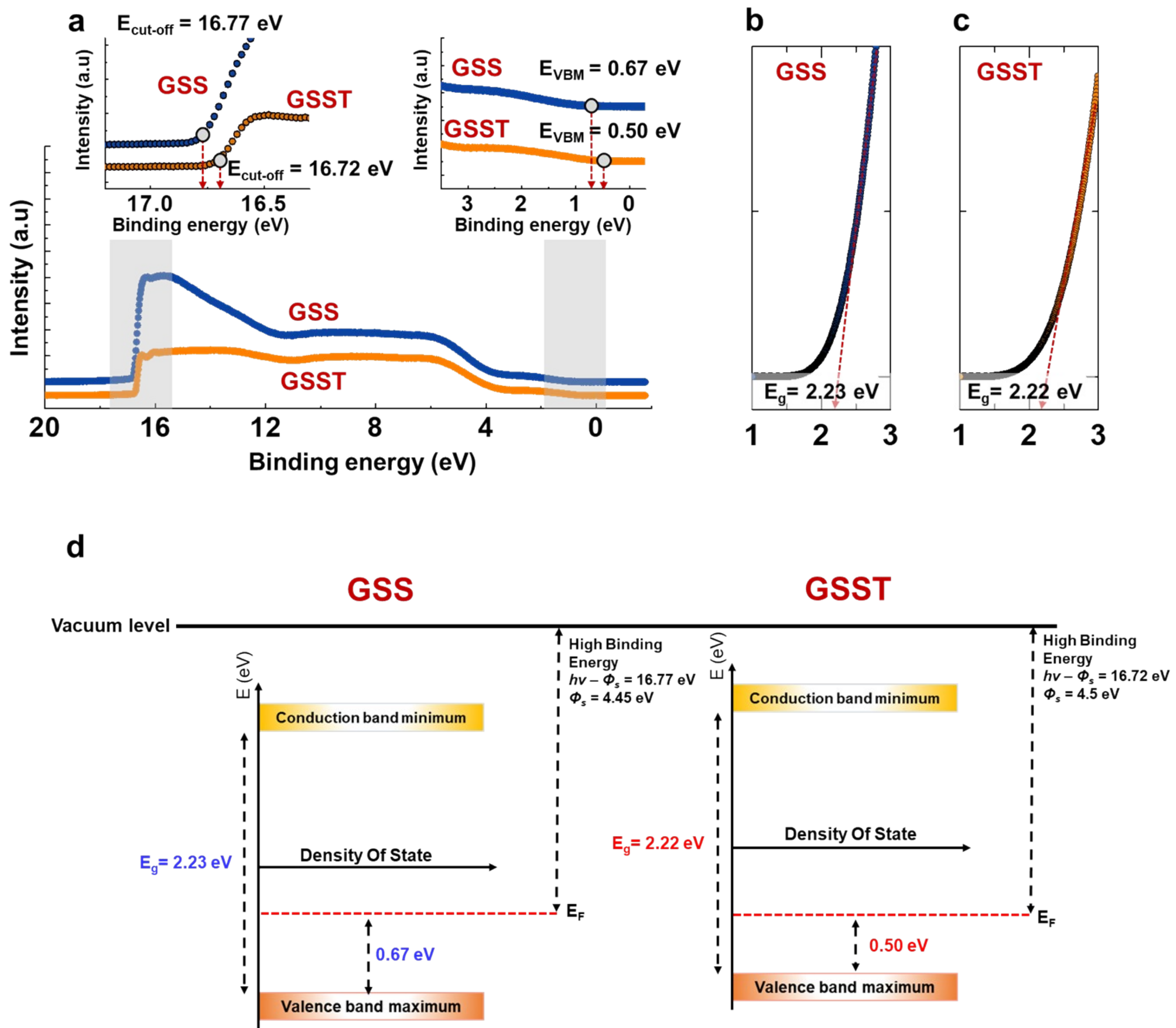

Fig. S5 (a) UPS spectroscopy measurement results for the GSS and GSST SOM devices. The work functions (Φ) of these active layers are estimated by the relationship between the incident beam energy and the cut-off energy, while the valence band maximums were derived through linear fitting in the low binding energy region. Tauc plot of $(\alpha h\nu)^2$ versus $h\nu$ for (b) GSS and (c) GSST. (d) The integrated energy band diagrams of GSS and GSST based on the information from UPS measurement and Tauc plot fitting.

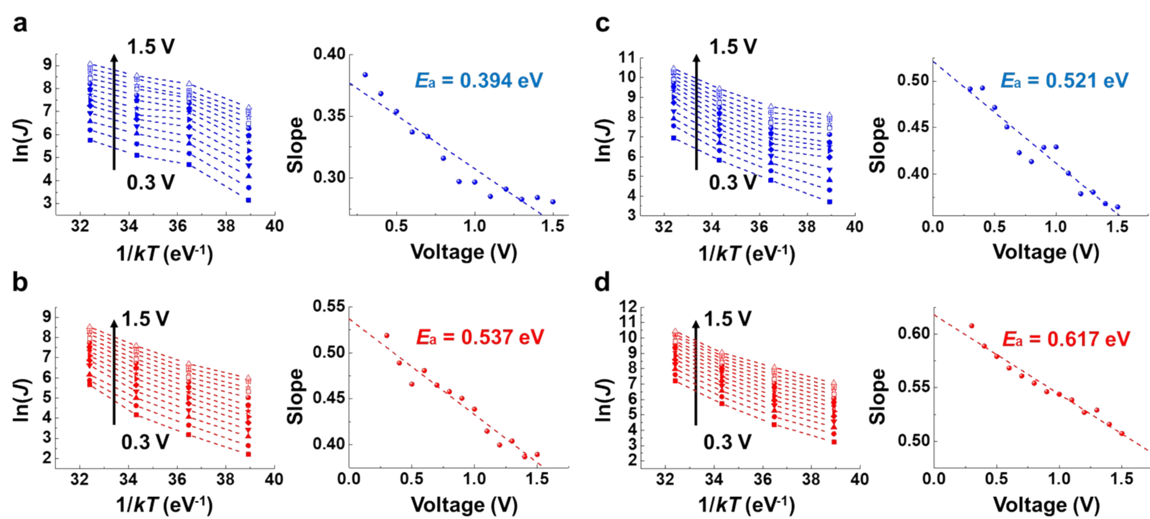

Fig. S6 Arrhenius plots for (a) GSS V_{th1}, (b) GSS V_{th2}, (c) GSST V_{th1}, and (d) GSST V_{th2} states.

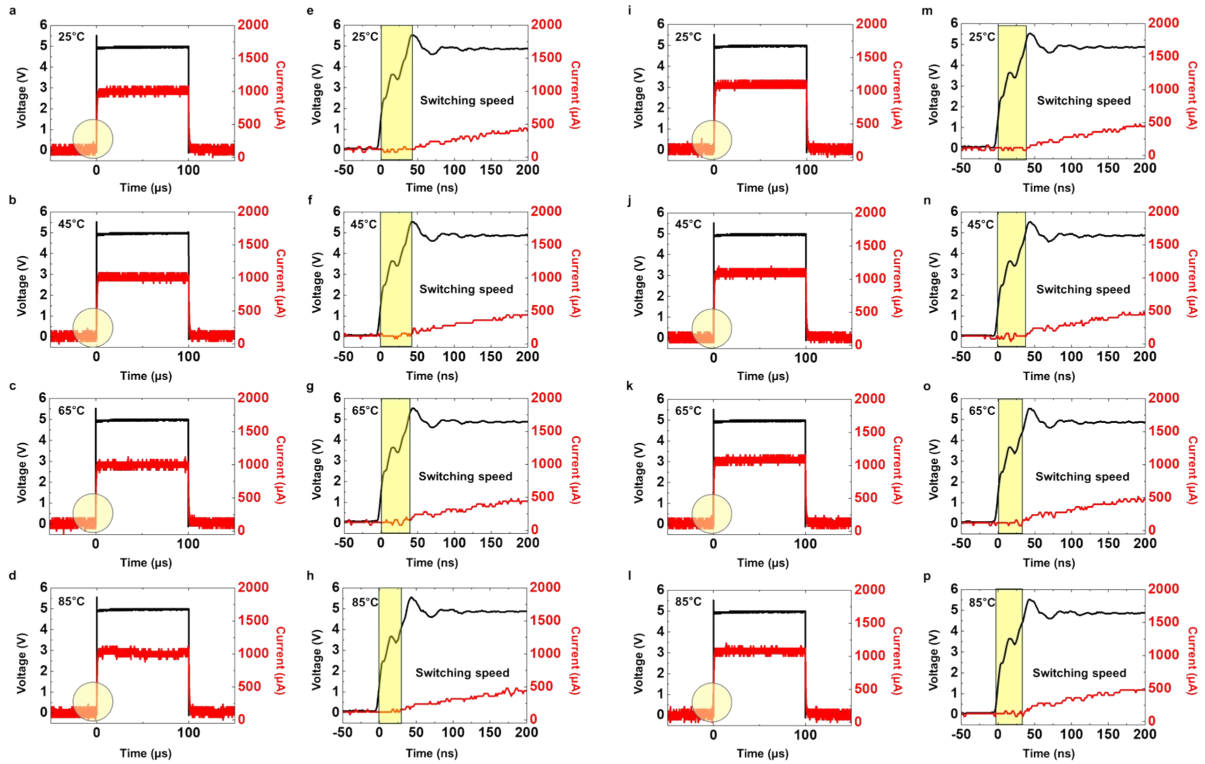

Fig. S7 Temperature-dependent transient current responses of the SOM devices. Transient current of the (a–d) GSS and (i–l) GSST devices measured at 25, 45, 65, and 85 °C, respectively, under a +5 V pulse (pulse width 100 μs, rise time 6 ns, fall time 6 ns), showing the occurrence of threshold switching (TS). Panels (e–h) (GSS) and (m–p) (GSST) present magnified views of the regions marked by yellow circles in (a–d) (GSS) and (i–l) (GSST), respectively, highlighting the abrupt current increase associated with the TS event. From the temperature-dependent measurements, the switching transition occurs within 50 ns for both materials at all temperatures, indicating an intrinsic switching speed below 50 ns independent of device type and temperature.

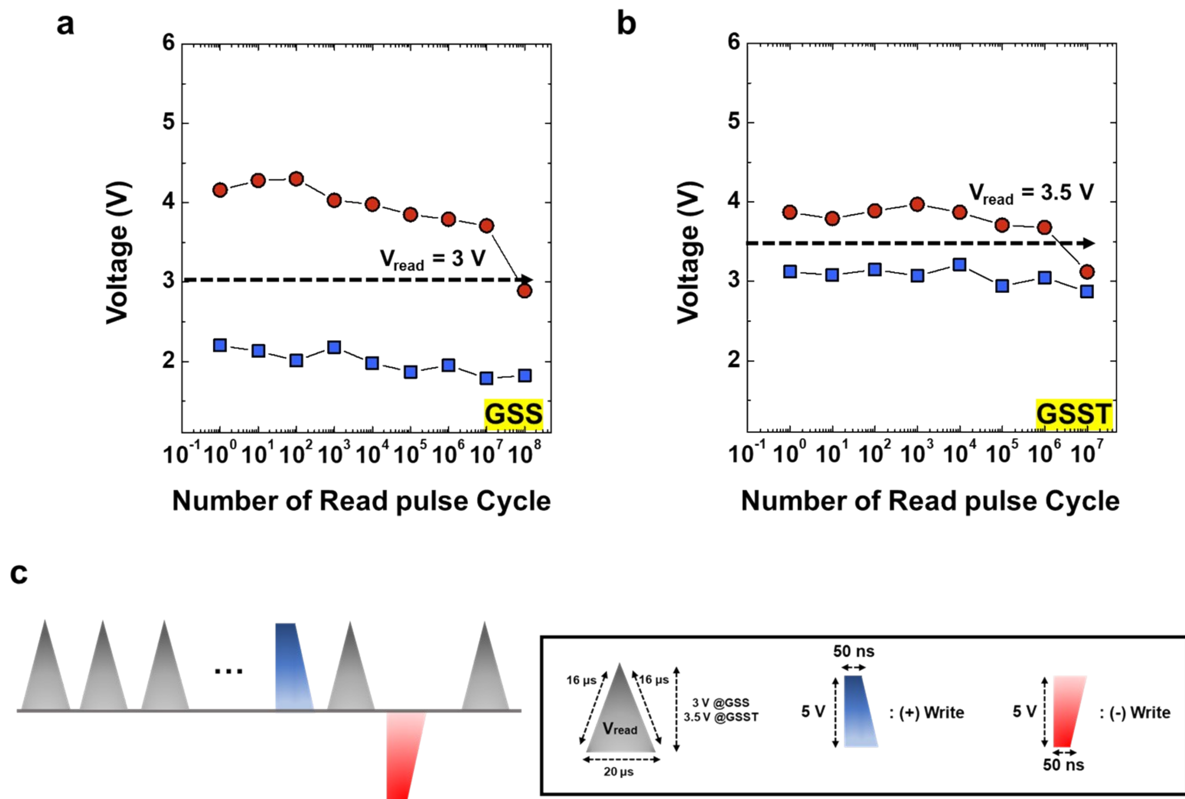

Fig. S8 Potential read disturb behavior of (a) GSS and (b) GSST SOM devices and (c) pulse scheme for read disturb measurement. Under the repeated read pulses with the amplitude of V_{read} (GSS @ 3 V, GSST @ 3.5 V), the devices exhibit the stable V_{th1} and V_{th2} over 10^7 cycles for GSS and 10^6 cycles for GSST.

Table S1 Homopolar and heteropolar bonds of Ge, Sb, Se, and Te, with corresponding bond energies, bond lengths, and electronegativities.

Bonding	Bonding energy (kcal/mol)	Bonding length (Å)	△Electronegativity (Pauling)
Ge–Ge	37.6[57]	2.45 ± 0.03[56]	0.0
Ge–Sb	33.7[57]	2.69 ± 0.02[58]	0.04
Ge–Se	49.1[57]	2.37 ± 0.03[56]	0.54
Ge–Te	35.5[57]	2.64 ± 0.02[58]	0.09
Sb–Sb	39.6[59]	2.44[58]	0.0
Sb–Se	43.9[57]	2.58 ~ 2.59[62]	0.5
Sb–Te	40.6[59]	2.83 ± 0.02[58]	0.05
Se–Se	44.0[57]	2.32 ± 0.03[56]	0.0
Se–Te	44.2[57]	2.57[60]	0.45
Te–Te	33.0[57]	2.76 ± 0.02[61]	0.0

Table S2 Performance comparison between our SOM and previous results.

Device case	This work		Sci. Rep. 2024[66]	IEDM 2023[40]	IEEE 2025[67]	IEDM 2023[68]	IEEE EDL 2025[69]
	GSS	GSST					
V_F (V)	~6.5	~6.5	~8	4.2	-	-	~6
RWM (V)	2.1	0.8	1.3	1.2	> 1	0.5	~3
T_{write} (s)	50 n	50 n	50 n(V_{th1}), 1 μ(V_{th2})	~10 n	10 μ	< 56 n	1 μ
Write pulse amplitude (V)	5	5	-	6	8	-	5
Write current (μA)	~10	~10	393(V_{th1}), 100(V_{th2})	< 100	-	40	75~300
V_{th1} / V_{th2} drift (mV/dec)	31 / 36.33	37.2 / 60.4	-	46.95 / 36.06	16 / 5	-	-
Retention	> 2 hr @ 85 °C	< 2 hr @ 85 °C	1 day @ 85 °C	> 10 years @ RT	-	-	10^3~10^5 s @ 85 °C
Endurance (cycles)	10^6	10^4	10^5	10^8	-	10^8	-